AGU PUBLICATIONS

Geophysical Research Letters

RESEARCH LETTER
10.1002/2017GL074117

Key Points:
- Projected drought risk under 1.5 and 2°C climates is quantified with a set of coupled climate model simulations and multiple drought metrics
- Risk of consecutive drought years shows little change in the U.S. SW and Central Plains but robust increases in Europe and the Mediterranean
- Limiting warming to 1.5°C may have benefits for future drought risk, but such benefits are regional and in some cases highly uncertain

Supporting Information:
- Supporting Information S1

Correspondence to:
F. Lehner,
flehner@ucar.edu

Citation:
Lehner, F., S. Coats, T. F. Stocker, A. G. Pendergrass, B. M. Sanderson, C. C. Raible, and J. E. Smerdon (2017), Projected drought risk in 1.5°C and 2°C warmer climates, *Geophys. Res. Lett.*, *44*, doi:10.1002/2017GL074117.

Received 12 MAY 2017
Accepted 6 JUL 2017
Accepted article online 7 JUL 2017

Projected drought risk in 1.5°C and 2°C warmer climates

Flavio Lehner[1], Sloan Coats[2], Thomas F. Stocker[3,4], Angeline G. Pendergrass[2], Benjamin M. Sanderson[2], Christoph C. Raible[3,4], and Jason E. Smerdon[5]

[1]Research Applications Laboratory, National Center for Atmospheric Research, Boulder, Colorado, USA, [2]Climate and Global Dynamics Laboratory, National Center for Atmospheric Research, Boulder, Colorado, USA, [3]Oeschger Centre for Climate Change Research, University of Bern, Bern, Switzerland, [4]Climate and Environmental Physics, University of Bern, Bern, Switzerland, [5]Lamont-Doherty Earth Observatory, Columbia University, Palisades, New York, USA

Abstract The large socioeconomic costs of droughts make them a crucial target for impact assessments of climate change scenarios. Using multiple drought metrics and a set of simulations with the Community Earth System Model targeting 1.5°C and 2°C above preindustrial global mean temperatures, we investigate changes in aridity and the risk of consecutive drought years. If warming is limited to 2°C, these simulations suggest little change in drought risk for the U.S. Southwest and Central Plains compared to present day. In the Mediterranean and central Europe, however, drought risk increases significantly for both 1.5°C and 2°C warming targets, and the additional 0.5°C of the 2°C climate leads to significantly higher drought risk. Our study suggests that limiting anthropogenic warming to 1.5°C rather than 2°C, as aspired to by the Paris Climate Agreement, may have benefits for future drought risk but that such benefits may be regional and in some cases highly uncertain.

Plain Language Summary Droughts are among the costliest natural disasters. It is therefore crucial to understand how drought risk will change in the future and whether climate mitigation might help reduce exposure to drought. We use a set of simulations with a climate model targeted at climates that are 1.5°C and 2°C warmer than the era before industrial development—the warming target in the Paris Climate Agreement—to investigate potential future drought risk. We find that drought risk increases across many regions of the world in both of these scenarios, by two different measures: general drying, as well as an increased frequency of consecutive dry years. In Europe, the Mediterranean, Amazon, and southern Africa, the 1.5°C warmer scenario has significantly lower drought risk than the 2°C scenario. In contrast to other simulations with much more warming, drought risk does not change significantly over the U.S. Central Plains and Southwest for these low warming scenarios. This study highlights that aggressive climate change mitigation might reduce future drought risk, but more research with other climate models is necessary to make sure these results are robust.

1. Introduction

Droughts are one of the costliest impacts of climate variability, but the factors controlling their onset and duration are still poorly understood [*Handmer et al.*, 2012]. Paleoclimate proxies and modeling studies indicate that severe multidecadal droughts can arise from internal climate variability alone, in the absence of strong external forcing [*Cook et al.*, 2007, 2016; *Hunt*, 2011; *Coats et al.*, 2016a; *Stevenson et al.*, 2015]. At the same time, evidence is accumulating that warming over recent decades may have affected the hydrologic cycle in semiarid regions [*Seager et al.*, 2007; *Kelley et al.*, 2015; *Lehner et al.*, 2017], potentially amplifying drought risk when precipitation deficits occur [*Diffenbaugh et al.*, 2015; *Williams et al.*, 2015]. Current research indicates that many historically drought-prone regions will face increased drought risk with continued anthropogenically driven global warming [*Held et al.*, 2005; *Dai*, 2011a; *Hoerling et al.*, 2012; *Fu and Feng*, 2014; *Prudhomme et al.*, 2014; *B. I. Cook et al.*, 2015; *Kelley et al.*, 2015; *Duffy et al.*, 2015; *Ault et al.*, 2016] and that this increase is robust across models since it is primarily driven by mean temperature change. However, there exist considerable uncertainties in observed and projected drought related to the choice of drought index, model structural differences, emissions scenarios, and internal variability [*Intergovernmental Panel on Climate Change*, 2012; *Burke and Brown*, 2008; *Sheffield et al.*, 2012; *Orlowsky and Seneviratne*, 2013; *Trenberth et al.*, 2014; *Scheff and Frierson*, 2015; *Smerdon et al.*, 2015; *Swann et al.*, 2016; *Berg et al.*, 2016; *Raible et al.*, 2017]. In particular, the risk of multidecadal "megadroughts" remains challenging to constrain, due to the long records needed [*Coats and Mankin*, 2016] and

the possibility that current climate models may underestimate low-frequency hydroclimate variability [*Ault et al*., 2013; *Smerdon et al*., 2017].

Recent decades have demonstrated that droughts lasting only a few years also pose significant socioeconomic risk, even when they are moderate in severity, because of their potential to deplete stored water quickly and thus to decrease resilience to subsequent droughts [*Howitt et al*., 2014; *Udall and Overpeck*, 2017; *Castle et al*., 2014]. Such consecutive moderate drought years also offer the opportunity for a more accurate assessment due to a lesser dependence on long records from observations and simulations. This accuracy might be particularly important for emissions scenarios with more subtle differences in warming than comparing business-as-usual to aggressive mitigation scenarios, e.g., Representative Concentration Pathway (RCP) 8.5 [*Taylor et al*., 2012] against RCP 2.6 or RCP 4.5 [*Ault et al*., 2016; *Lin et al*., 2016].

The goal of the Paris agreement is to hold global warming well below 2°C and to pursue efforts to limit to 1.5°C above preindustrial temperature. Regardless of the political and socioeconomic achievability of these goals [*Stocker*, 2013; *Sanderson et al*., 2017], it is important to quantify how drought risk changes for these two warming targets and whether there are significant differences between them. Such an assessment is currently hampered by a number of issues: (i) only a small number of existing simulations of the Coupled Model Intercomparison Project 5 (CMIP5) under the RCP 2.6 scenario result in a warming limited to 1.5°C by the end of the 21st century; (ii) new modeling efforts such as the "Half a degree Additional warming, Projections, Prognosis and Impacts" (HAPPI) model intercomparison project [*Mitchell et al*., 2016] will use prescribed climatological sea surface temperatures and hence will not include coupled ocean-atmosphere internal variability, which has been identified as crucial for simulating realistic drought variability and persistence [*Seager et al*., 2005; *Coats et al*., 2016a; *Routson et al*., 2016]; and (iii) when investigating the risk of consecutive drought years in a near-stable climate, a composite analysis of individual 20 year time slices selected from CMIP5 (e.g., following *Schleussner et al*. [2016] for other impacts at 1.5°C) may not be feasible due to insufficient sampling of extended drought events.

To overcome these issues and provide a first assessment of drought risk under the 1.5°C and 2°C warming targets, we use a set of ensemble simulations with the Community Earth System Model (CESM) designed specifically to test the climate impacts associated with 1.5°C and 2°C warming scenarios [*Sanderson et al*., 2017]. We assess meteorological drought defined by different forms of the Palmer Drought Severity Index and soil moisture (as opposed to drought defined by changes in vegetation or runoff). We focus on key drought-prone regions in North and South America, Europe, Africa, Asia, and Australia where we are relatively confident in CESM and our drought metrics to answer the following questions: (1) Do drought metrics, on average, change at 1.5°C and 2°C warming? (2) Does the risk for consecutive drought years change at 1.5°C and 2°C warming? (3) Are there significant differences between the two warming targets for these two questions?

2. Materials and Methods

2.1. Model Simulations

The coupled model simulations used in this study were designed specifically to enable investigation of impacts at near-equilibrium climates of 1.5°C and 2°C in the global mean above preindustrial temperatures [*Sanderson et al*., 2017]. The simulations use the Community Earth System Model (CESM) [*Hurrell et al*., 2013], with the same model version and setup as was used for the CESM Large Ensemble (CESM LE), and use the CESM LE preindustrial control simulation as baseline reference [*Kay et al*., 2015]. While model structural uncertainty is not represented in this study here, it is worth noting that in other studies, the mean response of drought in CESM to anthropogenic warming has been found to be similar to the CMIP5 multimodel mean [*Seneviratne et al*., 2013; *Cook et al*., 2014; *B. I. Cook et al*., 2015]. This single-model setup allows for a more robust sampling of internal variability than would be possible in CMIP5, where only a few models provide multiple ensemble members.

The complete description of the experimental setup of the simulations is provided in *Sanderson et al*. [2017] and summarized here. The Minimal Complexity Earth Simulator (MiCES) is used to emulate the coupled climate of CESM in a simplistic manner, making it computationally tractable to find greenhouse gas emission pathways that would lead CESM to a desired global mean temperature. The emission pathways derived

from MiCES are then used to force the first 10 ensemble members of CESM LE from 2006 to 2100. Nongreenhouse gas concentrations (aerosols, ozone, and CFCs) follow the RCP 8.5 protocol [*Taylor et al*., 2012] throughout the simulations, an assumption with little effect on the projection uncertainty given the generally small differences in aerosol forcing across RCPs [e.g., *Pendergrass et al*., 2015]. This results in two 10-member ensembles that stabilize at 1.5°C and 2°C of warming above preindustrial by 2050–2070 [*Sanderson et al*., 2017, Figure 1b]. For the reminder of the study, the 1.5°C and 2°C climates are therefore defined as the period 2051–2100 in each 10-member ensemble. We further use the existing simulations from the same 10 CESM LE members to define the present-day reference period 1967–2016 (0.35°C above preindustrial) and the future period 2051–2100 under RCP 8.5 (3.7°C above preindustrial).

2.2. Drought Metrics

To be consistent with previous studies of future drought, we use the annual mean Palmer Drought Severity Index (PDSI) [*Palmer*, 1965] with the Penman-Monteith formulation of potential evapotranspiration as a primary drought metric. PDSI is calculated off-line from CESM output following *Coats and Mankin* [2016], which entails a standardization of the PDSI index against the preindustrial control simulation, such that values of −2, −3, and −4 represent moderate, severe, and extreme drought at a given location (analogous to Palmer's original classification for the U.S. Midwest in the 1930s; see also *Dai* [2011b] for discussion). Thus, a future mean decrease by, e.g., one PDSI unit would represent an impactful drying. To provide a measure of real-world natural variability for comparison to the model simulations, we use tree ring based reconstructions of June–August (JJA) PDSI from the North American, Monsoon Asia, and Old World Drought Atlases, covering the common period 1110–2005 Common Era (C.E.), during which the spatial coverage of the atlases is stable [*Cook et al*., 2004, 2010; *E. R. Cook et al*., 2015]. The PDSI in the Drought Atlases is not entirely consistent with the model, as they employ a different standardization interval (~1931–1990 C.E.) and temporal averaging (June–August versus annual mean). Nevertheless, June–August PDSI is highly correlated with annual mean PDSI due to its inherent 12–18 month memory, and the mean PDSI is largely stable during the preindustrial period in the Drought Atlases despite the short historical standardization interval [e.g., *Coats et al*., 2016b].

To test whether the PDSI results are consistent with other off-line drought metrics, we also calculate PDSI using potential evapotranspiration (PET) based solely on surface radiation; i.e., PET is expressed as 0.8 times the net surface radiation [*Milly and Dunne*, 2016], hereafter called $PDSI_{net\text{-}rad}$. Furthermore, to test whether the PDSI results are consistent with online drought metrics, we also investigate changes in simulated soil moisture: soil moisture to a depth of ~30 and ~200 cm is extracted from CESM by integrating liquid and frozen soil moisture over the upper 6 and 9 soil levels in the Community Land Model and then normalized against values from the preindustrial control simulation (subtract mean and divide by standard deviation). This approach follows previous studies that have addressed the potential for an unrealistic sensitivity of Penman-Monteith-based PDSI to anthropogenic warming by exploring alternative metrics [*B. I. Cook et al*., 2015; *Milly and Dunne*, 2016; *Berg et al*., 2016; *Feng et al*., 2017].

3. Results

3.1. Mean Changes in Drought

We first investigate mean changes in PDSI from present day (1967–2016) and to each of the 1.5°C and 2°C scenarios in the second half of the 21th century (2051–2100), as well as from 1.5°C to 2°C (Figure 1). Statistical significance is evaluated with a two-sided *t* test at 95% confidence. The Mediterranean, central Europe, the Amazon, and southern Africa see widespread drying under both 1.5°C and 2°C climates (Figures 1a and 1b), with significantly more drying at 2°C compared to 1.5°C (Figure 1c). The United States (US) Southwest does not see significant drying relative to present day, while the eastern half of the Central Plains shows weak but significant drying under both scenarios. There are almost no differences, however, between 1.5°C and 2°C for both U.S. regions. Southeast Asia generally does not see significant differences in PDSI relative to present day, while southern Australia shows significant drying of statistically indistinguishable magnitude under both scenarios. These results are generally detectable in $PDSI_{net\text{-}rad}$ and soil moisture as well, although some differences are noteworthy (Figures S1–S3): central Europe sees decreases in $PDSI_{net\text{-}rad}$ and soil moisture of almost equal magnitude at 1.5°C and 2°C, while PDSI is distinct between the two climates. There is a similar tendency in southern Africa, where soil moisture changes indicate no clear distinction between the two scenarios, while both PDSI indices do. Also, parts of the U.S.

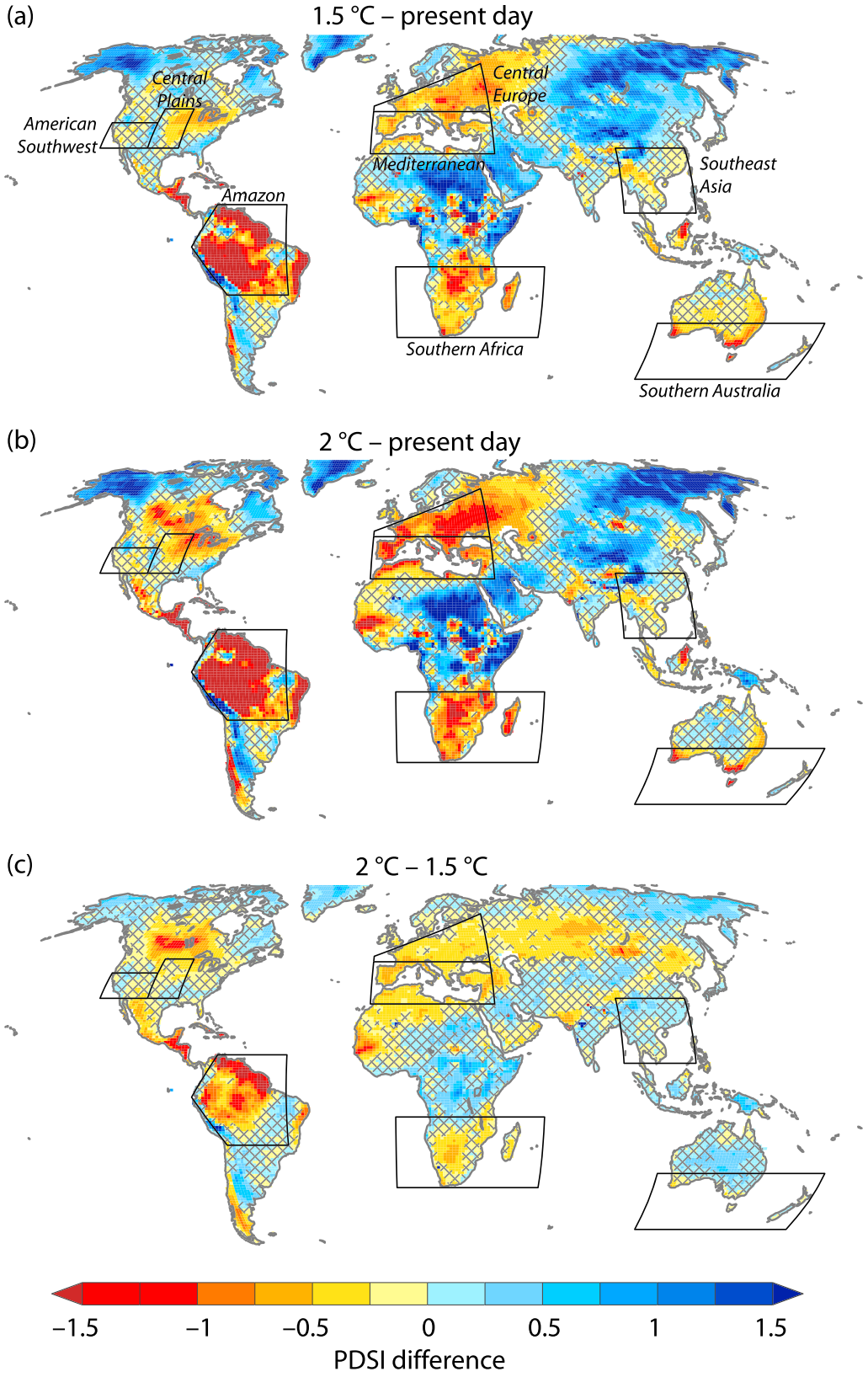

Figure 1. Change in mean PDSI (a) from present day (1967–2016) to 1.5°C (2051–2100), (b) from present day to 2°C (2051–2100), and (c) from 1.5°C to 2°C, as simulated by CESM. Hatching indicates differences that are not significant according to a two-sided *t* test (95% confidence). Boxes indicate regions used in Figures 2–4.

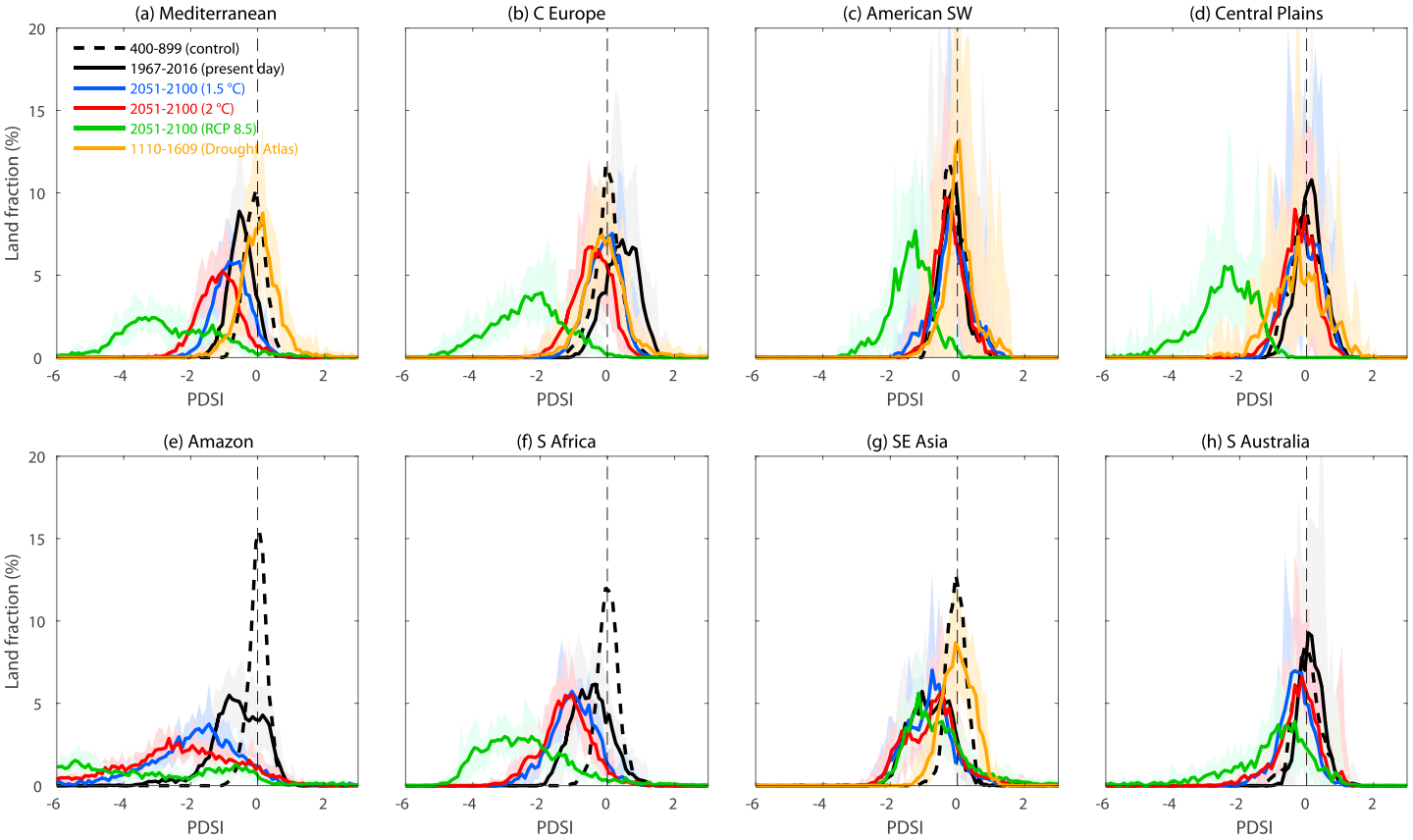

Figure 2. Fifty year mean PDSI from CESM simulations as a function of land fraction for the different regions marked in Figure 1. Also shown is the PDSI from the (a, b) Old World Drought Atlas [*E. R. Cook et al.*, 2015], (c, d) North American Drought Atlas [*Cook et al.*, 2004], and (g) Monsoon Asia Drought Atlas [*Cook et al.*, 2010] for regions where they provide coverage. Each thick solid line is the mean of the corresponding ten 50 year periods; the shading indicates the full range across those 10 values, omitted from the control for clarity. The ten 50 year periods represent the same time period for the simulations, while they represent 10 consecutive nonoverlapping 50 year periods between 1110 and 1609 in the case of the Drought Atlases.

Southwest see significantly reduced soil moisture at 1.5°C and 2°C, while PDSI shows an insignificant response. Generally, the two soil moisture metrics show comparable responses to 1.5°C and 2°C warming in CESM, unlike the depth gradient in soil moisture response reported for stronger warming scenarios in CMIP5 models [*Berg et al.*, 2016].

3.2. Spatially Aggregated Changes in Drought

In the context of a regional risk assessment, spatially aggregating mean changes is helpful to investigate the risk of a particular land fraction being impacted by climate change, rather than a specific grid cell [*Fischer et al.*, 2013]. That is, grid cells are binned according to their mean change and plotted against the land fraction that each bin makes up (Figure 2); significant changes in the mean of these spatial probability density functions are reported at 95% confidence based on a two-sided t test. Compared to spatially averaging, it also avoids the problem of erroneously averaging out opposing signals within a region. This is relevant for the U.S. Southwest and central Europe where the CMIP5 multimodel mean suggests opposing precipitation responses to strong warming (e.g., a north-south gradient) [*Intergovernmental Panel on Climate Change*, 2013]. In Figure 2 we show the spatially aggregated mean PDSI for 2051–2100 for the regions discussed in section 3.1. In addition to the model-simulated results from the 1.5°C and 2°C simulations, we also show the average PDSI from 10 independent 50 year periods (1110–1609) from the regional Drought Atlases. Where available, the Drought Atlases and the preindustrial control simulation show good agreement in terms of spatially aggregated PDSI (Figure S4 and accompanying discussion in the supporting information).

The spatially aggregated PDSI generally confirms what was shown in Figure 1: significant drying in the Mediterranean, central Europe, the Amazon, southern Africa, and southern Australia at 1.5°C and 2°C, and insignificant changes in the U.S. Southwest, Central Plains, and Southeast Asia (Figure 2). Compared to the colocated Drought Atlas during the last millennium and the preindustrial control simulation, the Mediterranean is drier at present in CESM, although the lowest values of the Drought Atlas distribution suggest that some land area and/or periods between 1110 and 1609 were as dry (Figure 2a). Central Europe, on the other hand, is wetter today in CESM than in any period in the Drought Atlas, while the 1.5°C climate over central Europe in CESM resembles the 1110–1609 period of the Drought Atlas most closely (Figure 2b). Future conditions in central Europe might therefore be similar to the preindustrial period (Figure S4b) or, assuming the model is unbiased relative to the reconstruction, similar to some periods in the paleoclimate record (Figure 2b). The present-day U.S. Southwest and Central Plains in CESM are largely indistinguishable from the Drought Atlas (Figures 2c and 2d). In Southeast Asia, the present-day climate is significantly drier than in the Drought Atlas and the simulated preindustrial period (Figure 2g). We speculate that this might be related to aerosol forcing [*Bollasina et al*., 2011; *Lin et al*., 2016].

To illustrate the benefits of limiting warming to 1.5°C or 2°C in terms of drought risk, we compare them with the RCP 8.5 projection (green lines in Figure 2), which is 3.7°C warmer than preindustrial in CESM. The U.S. Southwest and Central Plains dry significantly under RCP 8.5 (see also *B. I. Cook et al*. [2015] and others), yet almost none of this drying occurs at 1.5°C or 2°C warming. This behavior stands in stark contrast to the Mediterranean, central Europe, the Amazon, southern Africa, and southern Australia, where drying appears to scale more linearly with the level of warming. Southeast Asia experiences no change in PDSI with RCP 8.5 in CESM. As discussed in *Lin et al.* [2016], future reductions of aerosol concentrations in this region cause an increase in both precipitation and evaporative demand relative to simulations with fixed aerosol emissions. While increases in greenhouse gas concentrations also cause an increase in precipitation and evaporative demand, the resulting relative drying and wetting across the Southeast Asia region seems to cancel out [*Lin et al*., 2016]. However, a more detailed study of this region is warranted given the spatial and temporal complexity of its drought response.

To investigate the nonlinear scaling of the drying signal in the U.S. Southwest and Central Plains with temperature, we recalculate PDSI after detrending the model-simulated potential evapotranspiration (PET) (by removing a quadratic fit at each grid cell for the 1.5°C and 2°C scenarios, similar to removal of a linear fit for RCP 8.5 in *Cook et al*. [2014]). This approach essentially holds PET constant at preindustrial levels while retaining internal variability and isolates the response of PDSI to changes in precipitation alone. Figure S5 shows these calculations for the 1.5°C and 2°C scenarios alongside the original PDSI calculations from Figure 2, as well as PDSI from present day and the preindustrial control simulation. Figures S5a, S5e, and S5f illustrate that the precipitation decrease alone causes a substantial fraction of the drying from preindustrial to the 1.5°C and 2°C warmer climates in the Mediterranean (33–37%), the Amazon (53–59%), and southern Africa (70–84%), consistent with the robust regional pattern of strengthening of moisture divergence with global warming [*Held and Soden*, 2006; *Seager et al*., 2014; *Boisier et al*., 2015] (see also Figures S6a and S6b). The strengthening of moisture divergence with warming also causes increased moisture convergence over central Europe and leads to increased precipitation there [*Seager et al*., 2014] (see also S6 for maps of projected precipitation change); this would lead to increased PDSI (Figure S5b) were it not for the even larger increase in evaporative demand at 1.5°C and 2°C due to the temperature increase (Figures 2, S5b, S7, and S8). Over the U.S. Southwest and Central Plains, on the other hand, increased precipitation at 1.5°C and 2°C is almost exactly offset by increased evaporative demand, so that there is almost no change relative to preindustrial or present day (Figures S5c, S5d, S6, and S7). This balance does not hold for stronger warming, causing the U.S. Southwest and Central Plains to dry under RCP 8.5, which explains the nonlinear scaling of PDSI changes with warming in these regions. In southern Australia, precipitation is projected to increase more at 2°C than 1.5°C warming (Figure S5h), so that the combined effect of changes in precipitation and evaporative demand yields a drying of similar magnitude for the two warming targets (recall Figure 2h).

3.3. Risk of Consecutive Drought Years

We define a consecutive drought "event" as four consecutive years of negative PDSI whose cumulative sum is below −4. This threshold corresponds roughly to the recent 2012–2015 drought in California [e.g., *Griffin and Anchukaitis*, 2014; *Williams et al*., 2015], which had substantial socioeconomic impacts despite its relatively

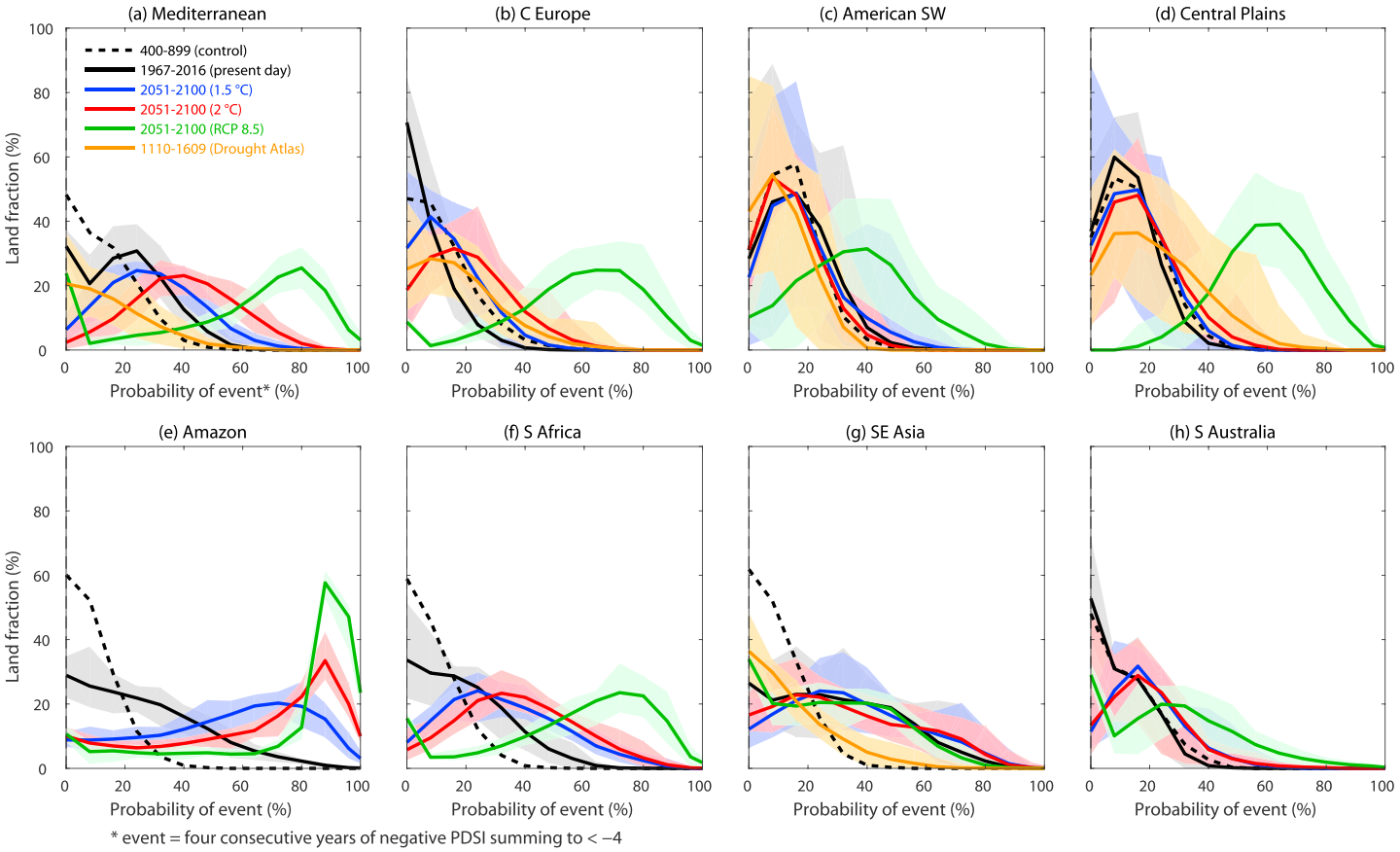

Figure 3. Spatially aggregated risk of four consecutive years of negative PDSI summing to less than −4 as a function of land fraction for the regions defined in Figure 1. Risk is defined as the probability of occurrence, i.e., the number of events divided by the maximum number of possible nonoverlapping events in a 50 year period. Shading indicates the full range across the 10 ensemble members, omitted from the control for clarity.

short duration. Other lengths of consecutive drought years (3 through 10) were tested as well, with similar results (not shown). Figure 3 shows the risk of a consecutive drought event during the years 2051–2100, expressed in terms of affected land fraction as a function of probability of an event for the eight regions. Probability is calculated as the number of events divided by 12, the maximum possible number of such nonoverlapping events in a given 50 year period.

The Mediterranean experiences substantially elevated risk of consecutive drought years at 1.5°C and 2°C compared to present day and even more so compared to the Drought Atlas (Figure 3a). There are also notable differences between the two scenarios; the land fraction with low risk (<10%) is reduced by half at 2°C compared to 1.5°C, while the land fraction with high risk (>60%) more than doubles. In central Europe, the risk of consecutive years of drought is generally lower, although a similar increase in risk occurs for a warming of 2°C relative to 1.5°C (Figure 3b). In contrast to the Mediterranean, in central Europe the Drought Atlas indicates that the risk of consecutive years of drought during the 1110–1609 period was similar to the risk estimated by CESM for 1.5°C and °C (suggesting that present day is wetter than either the past or the future). The risk of consecutive drought years in the U.S. Southwest and Central Plains does not change notably at 1.5°C and 2°C (Figures 3c and 3d). For the U.S. Southwest, the risk documented by the Drought Atlas is indistinguishable from the present day and 1.5°C and 2°C warming scenarios (Figure 3c). For the Central Plains, in contrast, the Drought Atlases document a higher risk of consecutive drought years than present day or the 1.5°C and 2°C scenarios (Figure 3d). The Amazon experiences the strongest response, with a complete shift of the distribution to higher risk (Figure 3e). Southern Africa experiences a response similar to the Mediterranean (Figure 3f). In line with its mean PDSI (Figure 2), Southeast Asia's risk for consecutive drought years does not change with any future scenario but is higher than documented by the Drought Atlas (Figure 3g). Southern Australia experiences an

increase in risk of consecutive drought years under both 1.5°C and 2°C scenarios relative to present day, with a strong reduction of the land fraction at low risk (<10%) and a corresponding increase in higher risk (Figure 3h); no notable differences exist between 1.5°C and 2°C.

Under RCP 8.5, the risk of consecutive drought years increases substantial in all regions except Southeast Asia. Note that the period 2051–2100 is still warming unabated in RCP 8.5, thus only allowing a qualitative comparison of RCP 8.5 with the 1.5°C and 2°C simulations.

Most of the change in risk of consecutive drought years quantified with PDSI are consistent with those using $PDSI_{net\text{-}rad}$ and soil moisture (Figures S9–S11). Nonetheless, there are some differences; the relative response to warming is weaker, which is potentially related to the stronger temperature sensitivity of PDSI compared to $PDSI_{net\text{-}rad}$ and soil moisture. Especially in extratropical regions, where future drying is largely driven by increased evaporative demand, $PDSI_{net\text{-}rad}$ indicates less drying, consistent with observations [*van der Schrier et al*., 2013]. The risk of consecutive drought years in $PDSI_{net\text{-}rad}$ and soil moisture metrics decreases in Southeast Asia under RCP 8.5, in contrast to PDSI, which shows no change under RCP 8.5 relative to present day. Again, this seems to be related to the stronger sensitivity of PDSI to temperature compared to the other metrics, as Southeast Asia has strong increases in precipitation under RCP 8.5 as a consequence of projected mitigation of aerosol emissions and associated warming [*Lin et al*., 2016] that are balanced by increasing evaporative demand. This latter response appears to be weaker for $PDSI_{net\text{-}rad}$ and simulated soil moisture than for PDSI.

4. Summary and Conclusions

Using a set of coupled simulations with CESM [*Sanderson et al*., 2017], we provide an assessment of drought for 1.5°C and 2°C warmer climates, including mean changes as well as the risk of consecutive years of moderate drought. Our analysis indicates that when warming is limited to 1.5°C or 2°C, projected increases in precipitation and temperature/evaporative demand may balance each other over the U.S. Southwest and Central Plains, leading to little change in drought risk relative to present day (and in contrast to the dramatic increase in projected drought risk with the business-as-usual RCP 8.5 scenario). In the Mediterranean, central Europe, the Amazon, and southern Africa, on the other hand, drought risk increases significantly for both warming targets. Moreover, for these four regions the additional 0.5°C of warming from 1.5°C to 2°C leads to significantly drier mean conditions and higher risk of consecutive drought years. Southern Australia has a comparable increase in drought risk between 1.5°C and 2°C, while Southeast Asia sees no significant change in drought risk under any future scenario.

The nonlinear scaling of drought risk over the U.S. Southwest and Central Plains is complex, as it suggests that the assessment of impacts at 1.5°C and 2°C climates cannot simply be derived from pattern scaling, illustrating the limitations of pattern scaling as discussed in *Tebaldi and Arblaster* [2014]. The nonlinear scaling of drought risk with warming could provide motivation for climate change mitigation, as the costs associated with drought could scale nonlinearly too; cost-benefit analyses could consequently favor immediate over delayed mitigation, a topic that deserves further study. The balance between precipitation and evaporative demand that causes PDSI to remain stable in these regions is uncertain, however, as soil moisture in the same regions shows a more linear decrease with warming. Likewise, a recent statistical assessment of the drought risk in the U.S. Southwest suggested that in absence of precipitation increases of at least 10%, megadrought risk will rise sharply even under low warming [*Ault et al*., 2016]. A precipitation change of this magnitude is roughly what CESM simulates over the U.S. Southwest, and because regional precipitation projections are uncertain [*Simpson et al*., 2015], the results derived from just one model should be compared against projections with other models. Also, while the drying over Europe is robust among the different drought indices considered here and across models [*Seager et al*., 2014], differences between 1.5°C and 2°C are less robust across drought metrics. In the context of impacts assessment for low warming targets, it is noteworthy that our analysis shows significant discrepancies between drought indices under the strong warming of RCP 8.5 [e.g., *Feng et al*., 2017], while the responses are more consistent for 1.5°C and 2°C. Due to biases inherent in a single-model study and the generally poor observational constraint on drought risk [e.g., *Dirmeyer et al*., 2016], we urge caution when interpreting the results presented herein. Finally, although CESM has been found to behave similar to the CMIP5 mean in terms of drought responses to warming, the large structural uncertainty in future drought risk is not sampled in this single-model study. Coupled simulations of low

warming targets with other climate models are therefore needed to enable evaluation of the robustness of changes in drought across models.

Notwithstanding the caveats discussed above, our analysis indicates that climates stabilized at 1.5°C or 2°C warming above preindustrial temperatures could see increased drought risk relative to today in a number of populated areas of the world and that mitigation of warming by 0.5°C might yield significant reductions in exposure for some regions.

Acknowledgments
We acknowledge the efforts of all those who contributed to producing the CESM LE and the Drought Atlases. The CESM simulations are available on the Earth System Grid (www.earthsystemgrid.org); the Drought Atlases are available at National Oceanic and Atmospheric Administration (NOAA) Paleoclimatology (www.ncdc.noaa.gov/data-access/paleoclimatology-data/datasets). The National Center for Atmospheric Research is sponsored by the National Science Foundation. F.L. is supported by a Postdoc Applying Climate Expertise (PACE) fellowship cosponsored by NOAA and the Bureau of Reclamation. B.M.S. and A.G.P. are supported by the Regional and Global Climate Modeling Program of the U.S. Department of Energy's Office of Science, Cooperative Agreement [DE-FC02-97ER62402]. T.F.S. and C.C.R. acknowledge support by the Swiss National Science Foundation. J.E.S. supported in part by grants AGS-1243204 and AGS-1401400 from the U.S. This research was supported in part by NSF EaSM grant AGS 1243125 National Science Foundation. Lamont contribution number 8129.

References

Ault, T. R., J. E. Cole, J. T. Overpeck, G. T. Pederson, S. S. George, B. Otto-Bliesner, C. A. Woodhouse, and C. Deser (2013), The continuum of hydroclimate variability in western North America during the last millennium, *J. Clim.*, *26*, 5863–5878, doi:10.1175/JCLI-D-12-00732.1.

Ault, T. R., J. S. Mankin, B. I. Cook, and J. E. Smerdon (2016), Relative impacts of mitigation, temperature, and precipitation on 21st-century megadrought risk in the American Southwest, *Sci. Adv.*, *2*, 1–9, doi:10.1126/sciadv.1600873.

Berg, A., J. Sheffield, and P. C. D. Milly (2016), Divergent surface and total soil moisture projections under global warming, *Geophys. Res. Lett.*, 236–244, doi:10.1002/2016GL071921.

Boisier, J. P., P. Ciais, A. Ducharne, and M. Guimberteau (2015), Projected strengthening of Amazonian dry season by constrained climate model simulations, *Nat. Clim. Change*, *5*, 656–660, doi:10.1038/nclimate2658.

Bollasina, M. A., Y. Ming, and V. Ramaswamy (2011), Anthropogenic aerosols and the weakening of the south Asian summer monsoon, *Science*, *334*, 502–505, doi:10.1126/science.1204994.

Burke, E. J., and S. J. Brown (2008), Evaluating uncertainties in the projection of future drought, *J. Hydrometeorol.*, *9*, 292–299, doi:10.1175/2007JHM929.1.

Castle, S. L., B. F. Thomas, J. T. Reager, M. Rodell, S. C. Swenson, and J. S. Famiglietti (2014), Groundwater depletion during drought threatens future water security of the Colorado River Basin, *Geophys. Res. Lett.*, doi:10.1002/2014GL061055.

Coats, S., and J. S. Mankin (2016), The challenge of accurately quantifying future megadrought risk in the American Southwest, *Geophys. Res. Lett.*, *43*, 9225–9233, doi:10.1002/2016GL070445.

Coats, S., J. E. Smerdon, B. I. Cook, R. Seager, E. R. Cook, and K. J. Anchukaitis (2016a), Internal ocean-atmosphere variability drives megadroughts in Western North America, *Geophys. Res. Lett.*, *43*, 9886–9894, doi:10.1002/2016GL070105.

Coats, S., J. E. Smerdon, K. B. Karnauskas, and R. Seager (2016b), The improbable but unexceptional occurrence of megadrought clustering in the American West during the Medieval Climate Anomaly, *Environ. Res. Lett.*, *11*, 74025, doi:10.1088/1748-9326/11/7/074025.

Cook, B. I., J. E. Smerdon, R. Seager, and S. Coats (2014), Global warming and 21st century drying, *Clim. Dyn.*, *43*(9–10), 2607–2627.

Cook, B. I., T. R. Ault, and J. E. Smerdon (2015), Unprecedented 21st century drought risk in the American Southwest and Central Plains, *Sci. Adv.*, *1*, e1400082, doi:10.1126/sciadv.1400082.

Cook, B. I., E. R. Cook, J. E. Smerdon, R. Seager, A. P. Williams, S. Coats, D. W. Stahle, and J. V. Díaz (2016), North American megadroughts in the Common Era: Reconstructions and simulations, *Wiley Interdiscip. Rev. Clim. Change*, *7*, 411–432, doi:10.1002/wcc.394.

Cook, E. R., C. A. Woodhouse, C. M. Eakin, D. M. Meko, and D. W. Stahle (2004), Long-term aridity changes in the western United States, *Science*, *306*, 1015–1018, doi:10.1126/science.1102586.

Cook, E. R., R. Seager, M. A. Cane, and D. W. Stahle (2007), North American drought: Reconstructions, causes, and consequences, *Earth-Sci. Rev.*, *81*, 93–134, doi:10.1016/j.earscirev.2006.12.002.

Cook, E. R., K. J. Anchukaitis, B. M. Buckley, R. D. D'Arrigo, G. C. Jacoby, and W. E. Wright (2010), Asian monsoon failure and megadrought during the last millennium, *Science*, *328*, 486–489, doi:10.1126/science.1185188.

Cook, E. R., et al. (2015), Old World megadroughts and pluvials during the Common Era, *Sci. Adv.*, *1*, e1500561–e1500561, doi:10.1126/sciadv.1500561.

Dai, A. (2011a), Drought under global warming: A review, *Wiley Interdiscip. Rev. Clim. Change*, *2*, 45–65, doi:10.1002/wcc.81.

Dai, A. (2011b), Characteristics and trends in various forms of the Palmer Drought Severity Index during 1900–2008, *J. Geophys. Res.*, *116*, D12115, doi:10.1029/2010JD015541.

Diffenbaugh, N. S., D. L. Swain, and D. Touma (2015), Anthropogenic warming has increased drought risk in California, *Proc. Natl. Acad. Sci. U.S.A.*, *112*, 3931–3936, doi:10.1073/pnas.1422385112.

Dirmeyer, P. A., et al. (2016), Confronting weather and climate models with observational data from soil moisture networks over the United States, *J. Hydrometeorol.*, *17*, 1049–1067, doi:10.1175/JHM-D-15-0196.1.

Duffy, P. B., P. Brando, G. P. Asner, and C. B. Field (2015), Projections of future meteorological drought and wet periods in the Amazon, *Proc. Natl. Acad. Sci. U.S.A.*, *112*, 13,172–13,177, doi:10.1073/pnas.1421010112.

Feng, S., M. Trnka, M. Hayes, and Y. Zhang (2017), Why do different drought indices show distinct future drought risk outcomes in the U.S. Great Plains?, *J. Clim.*, *30*, 265–278, doi:10.1175/JCLI-D-15-0590.1.

Fischer, E. M., U. Beyerle, and R. Knutti (2013), Robust spatially aggregated projections of climate extremes, *Nat. Clim. Change*, *3*, 1033–1038, doi:10.1038/nclimate2051.

Fu, Q., and S. Feng (2014), Responses of terrestrial aridity to global warming, *J. Geophys. Res. Atmos.*, *119*, 7863–7875, doi:10.1002/2014JD021608.

Griffin, D., and K. J. Anchukaitis (2014), How unusual is the 2012–2014 California drought?, *Geophys. Res. Lett.*, *41*, 9017–9023, doi:10.1002/2014GL062433.1.

Handmer, J., et al. (2012), Changes in impacts of climate extremes: Human systems and ecosystems, Managing the Risks of Extreme Events and Disasters to Advance Climate Change Adaptation: IPCC Special Report, 231–290.

Held, I. M., and B. J. Soden (2006), Robust responses of the hydrological cycle to global warming, *J. Clim.*, *19*, 5686–5699.

Held, I. M., T. L. Delworth, J. Lu, K. L. Findell, and T. R. Knutson (2005), Simulation of Sahel drought in the 20th and 21st centuries, *Proc. Natl. Acad. Sci. U.S.A.*, *103*, 17,891–17,896, doi:10.1073/pnas.0509057102.

Hoerling, M., J. Eischeid, J. Perlwitz, X. Quan, T. Zhang, and P. Pegion (2012), On the increased frequency of Mediterranean drought, *J. Clim.*, *25*, 2146–2161, doi:10.1175/JCLI-D-11-00296.1.

Howitt, R., J. Medellín-azuara, and D. Macewan (2014), *Economic Analysis of the 2014 Drought for California Agriculture*, pp. 1–15, Cent. Watershed Sci. Univ. California, Davis, Calif. [Available at http://watershed.ucdavis.edu.]

Hunt, B. G. (2011), Global characteristics of pluvial and dry multi-year episodes, with emphasis on megadroughts, *Int. J. Climatol.*, *31*, 1425–1439, doi:10.1002/joc.2166.

Hurrell, J. W., et al. (2013), The community earth system model: A framework for collaborative research, *Bull. Am. Meteorol. Soc.*, *94*, 1339–1360, doi:10.1175/BAMS-D-12-00121.1.

Intergovernmental Panel on Climate Change (2012), Summary for policymakers, in *Managing the Risks of Extreme Events and Disasters to Advance Climate Change Adaptation*, pp. 487–542, Cambridge Univ. Press, Cambridge, U. K., and New York. [Available at http://www.scopus.com/inward/record.url?eid=2-s2.0-84928051547&partnerID=tZOtx3y1.]

Intergovernmental Panel on Climate Change (2013), Summary for policymakers, in *Climate Change 2013: The Physical Science Basis. Contribution of Working Group I to the Fifth Assessment Report of the Intergovernmental Panel on Climate Change*, pp. 1–29, Cambridge Univ. Press, Cambridge, U. K., and New York.

Kay, J. E., et al. (2015), The community earth system model (CESM) large ensemble project: A community resource for studying climate change in the presence of internal climate variability, *Bull. Am. Meteorol. Soc.*, *96*, 1333–1349, doi:10.1175/BAMS-D-13-00255.1.

Kelley, C. P., S. Mohtadi, M. A. Cane, R. Seager, and Y. Kushnir (2015), Climate change in the fertile crescent and implications of the recent Syrian drought, *Proc. Natl. Acad. Sci. U.S.A.*, *112*, 3241–3246, doi:10.1073/pnas.1421533112.

Lehner, F., E. R. Wahl, A. W. Wood, D. Blatchford, and D. Llewellyn (2017), Assessing recent declines in Upper Rio Grande River runoff efficiency from a paleoclimate perspective, *Geophys. Res. Lett.*, *44*, 4124–4133, doi:10.1002/2017GL073253.

Lin, L., A. Gettelman, Q. Fu, and Y. Xu (2016), Simulated differences in 21st century aridity due to different scenarios of greenhouse gases and aerosols, *Clim. Change*, 1–16, doi:10.1007/s10584-016-1615-3.

Milly, P. C. D., and K. A. Dunne (2016), Potential evapotranspiration and continental drying, *Nat. Clim. Change*, *6*, 6, doi:10.1038/NCLIMATE3046.

Mitchell, D., et al. (2016), Half a degree Additional warming, Projections, Prognosis and Impacts (HAPPI): Background and experimental design, *Geosci. Model Dev. Discuss.*, 1–17, doi:10.5194/gmd-2016-203.

Orlowsky, B., and S. I. Seneviratne (2013), Elusive drought: Uncertainty in observed trends and short-and long-term CMIP5 projections, *Hydrol. Earth Syst. Sci.*, *17*, 1765–1781, doi:10.5194/hess-17-1765-2013.

Palmer, W. C. (1965), Meteorological drought, U.S. Weather Bur. Res. Pap. No. 45, 58 pp.

Pendergrass, A. G., F. Lehner, B. M. Sanderson, and Y. Xu (2015), Does extreme precipitation intensity depend on the emissions scenario?, *Geophys. Res. Lett.*, *42*, 8767–8774, doi:10.1002/2015GL065854.

Prudhomme, C., et al. (2014), Hydrological droughts in the 21st century, hotspots and uncertainties from a global multimodel ensemble experiment, *Proc. Natl. Acad. Sci. U.S.A.*, *111*, 3262–3267, doi:10.1073/pnas.1222473110.

Raible, C. C., O. Bärenbold, and J. J. Gómez-Navarro (2017), Drought indices revisited— Improving and testing of drought indices in a simulation of the last two millennia for Europe, *Tellus A*, *69*, 1–15, doi:10.1080/16000870.2017.1296226.

Routson, C. C., C. A. Woodhouse, J. T. Overpeck, J. L. Betancourt, and N. P. McKay (2016), Teleconnected ocean forcing of Western North American droughts and pluvials during the last millennium, *Quat. Sci. Rev.*, *146*, 238–250, doi:10.1016/j.quascirev.2016.06.017.

Sanderson, B. M., et al. (2017), Community climate simulations to assess avoided impacts in 1.5 and 2 degree futures, *Earth Syst. Dyn. Discuss.*, doi:10.5194/esd-2017-42.

Scheff, J., and D. M. W. Frierson (2015), Terrestrial aridity and its response to greenhouse warming across CMIP5 climate models, *J. Clim.*, *28*, 5583–5600, doi:10.1175/JCLI-D-14-00480.1.

Schleussner, C. F., et al. (2016), Differential climate impacts for policy-relevant limits to global warming: The case of 1.5 °C and 2 °C, *Earth Syst. Dyn.*, *7*, 327–351, doi:10.5194/esd-7-327-2016.

Seager, R., Y. Kushnir, C. Herweijer, N. Naik, and J. Velez (2005), Modeling of tropical forcing of persistent droughts and pluvials over western North America: 1856–2000, *J. Clim.*, *18*, 4065–4088, doi:10.1175/JCLI3522.1.

Seager, R., et al. (2007), Model projections of an imminent transition to a more arid climate in southwestern North America, *Science*, *316*, 1181–1184, doi:10.1126/science.1139601.

Seager, R., H. Liu, N. Henderson, I. Simpson, C. Kelley, T. Shaw, Y. Kushnir, and M. Ting (2014), Causes of increasing aridification of the mediterranean region in response to rising greenhouse gases, *J. Clim.*, *27*, 4655–4676, doi:10.1175/JCLI-D-13-00446.1.

Seneviratne, S. I., et al. (2013), Impact of soil moisture-climate feedbacks on CMIP5 projections: First results from the GLACE-CMIP5 experiment, *Geophys. Res. Lett.*, *40*, 5212–5217, doi:10.1002/grl.50956.

Sheffield, J., E. F. Wood, and M. L. Roderick (2012), Little change in global drought over the past 60 years, *Nature*, *491*, 435–438, doi:10.1038/nature11575.

Simpson, I. R., R. Seager, M. Ting, and T. A. Shaw (2015), Causes of change in Northern Hemisphere winter meridional winds and regional hydroclimate, *Nat. Clim. Change*, *6*, doi:10.1038/NCLIMATE2783.

Smerdon, J. E., B. I. Cook, E. R. Cook, and R. Seager (2015), Bridging past and future climate across paleoclimatic reconstructions, observations and models: A hydroclimate case study, *J. Clim.*, *28*, 3212–3231, doi:10.1175/JCLI-D-14-00417.1.

Smerdon, J. E., et al. (2017), Comparing proxy and model estimates of hydroclimate variability and change over the Common Era, *Clim. Past Discuss.*, 1–70, doi:10.5194/CP-2017-37.

Stevenson, S., A. Timmermann, Y. Chikamoto, S. Langford, and P. Dinezio (2015), Stochastically generated north American megadroughts, *J. Clim.*, *28*, 1865–1880, doi:10.1175/JCLI-D-13-00689.1.

Stocker, T. F. (2013), The closing door of climate targets, *Science*, *339*, 280–282, doi:10.1126/science.1232468.

Swann, A. A. L. S., F. M. Hoffman, C. D. Koven, and J. T. Randerson (2016), Plant responses to increasing CO_2 reduce estimates of climate impacts on drought severity, *Proc. Natl. Acad. Sci. U.S.A.*, *113*, 10,019–10,024, doi:10.1073/pnas.1604581113.

Taylor, K. E., R. J. Stouffer, and G. A. Meehl (2012), An overview of CMIP5 and the experiment design, *Bull. Am. Meteorol. Soc.*, *93*, 485–498, doi:10.1175/BAMS-D-11-00094.1.

Tebaldi, C., and J. M. Arblaster (2014), Pattern scaling: Its strengths and limitations, and an update on the latest model simulations, *Clim. Change*, *122*, 459–471, doi:10.1007/s10584-013-1032-9.

Trenberth, K. E., A. Dai, G. van der Schrier, P. D. Jones, J. Barichivich, K. R. Briffa, and J. Sheffield (2014), Global warming and changes in drought, *Nat. Clim. Change*, *4*, 17–22, doi:10.1038/nclimate2067.

Udall, B., and J. Overpeck (2017), The 21st century Colorado River hot drought and implications for the future, *Water Resour. Res.*, doi:10.1002/2016WR019638.

van der Schrier, G., J. Barichivich, K. R. Briffa, and P. D. Jones (2013), A scPDSI-based global data set of dry and wet spells for 1901–2009, *J. Geophys. Res. Atmos.*, *118*, 4025–4048, doi:10.1002/jgrd.50355.

Williams, A. P., R. Seager, J. T. Abatzoglou, B. I. Cook, J. E. Smerdon, and E. R. Cook (2015), Contribution of anthropogenic warming to California drought during 2012–2014, *Geophys. Res. Lett.*, *42*, 6819–6828, doi:10.1002/2015GL064924.